Damping Behavior of Sandwich Beam Laminated with CIIR/Petroleum Resins Blends by DMA Measurement

Cong Li, Guozhang Wu, Fangyi Xiao, Chifei Wu

Polymer Alloy Laboratory, School of Materials Science and Engineering, East China University of Science and Technology, Shanghai 200237, People's Republic of China

Received 9 February 2006; accepted 19 June 2006
DOI 10.1002/app.25450
Published online 27 July 2007 in Wiley InterScience (www.interscience.wiley.com).

ABSTRACT: In this paper, we tried to develop a high damping material with chlorinated butyl rubber (CIIR) and petroleum resins. It was found that the addition of petroleum resins in CIIR could largely increase the loss factor and broaden the damping range. So a sandwich beam laminated with the new developed material was prepared, and the damping behavior of this sandwich beam was measured by dynamic mechanical analysis (DMA). The influence of temperature, frequency, thickness, and component of damping layer on the structural loss factor η_s determined by DMA was discussed based on a theoretical model. © 2007 Wiley Periodicals, Inc. J Appl Polym Sci 106: 2472–2478, 2007

Key words: damping behavior; dynamic mechanical property; chlorinated butyl rubber

INTRODUCTION

Polymers have been widely used for noise and vibration control in recent years. Many approaches for broadening the glass transition temperature (T_g) of the polymer so as to improve the effective damping range have been investigated. One of the most conventional ways is to mix several kinds of polymers with different T_g[1–3]; Interpenetrating polymer network (IPN) in which the phase-separated domain is limited to a very small size has been conformed to be a very effective structure as high-performance damping materials[4,5]; Addition of inorganic filler in polymer matrix is also a quite useful method to improve the damping behavior due to the friction between the filler and the chains of polymer.[3,6] Recently, a new concept based on hybrid of a bifunctional small molecule with a polar polymer was proposed by Wu for controlling the microphase separation and crystallization of the added small molecules in the polymer matrix.[7–10] Not only the loss peak is improved, but also the effective damping range is broadened.

In practical application, the polymeric damping materials are always laminated with other stiff sheets such as steel and aluminum. There are two main forms of damping treatments. One is extensional damping referred to as the free-layer damping treatment. The other is shear damping referred to as the constrained-layer damping treatment. Generally, the vibration damping properties of laminated beams can not be measured directly but instead are deduced from the response characteristics of them.[11] One measure of damping, known as the logarithmic decrement, is related to the ratio of the nth to the $n+N$th cycle amplitudes of a cantilever beam, which is deformed and then released from rest. The other method is the standard ASTM E 756-98, which is the common method of measuring the vibration damping property of a beam. The loss factor can be calculated around each resonance peak using the half-power bandwidth method.[12,13] It should be pointed out that determination of the vibration damping behavior by these methods requires specialized and complicated measuring system, and the measurement is very expensive.

The objective of this paper is to provide a simpler and cheaper method for investigating the damping behaviors of sandwich beams and to develop an optimized sandwich beam structure having a high damping property around room temperature at a frequency of 200 Hz. This work consists of three parts. Firstly, we developed a new kind of blends with high-damping performance and self-adhesive characteristic suitable as the damping layer of a sandwich beam; Secondly, dynamic mechanical analyzer (DMA) was used to measure the vibration damping behaviors of sandwich beams; Finally, a theoretical model was established to simulate the vibration damping behaviors of sandwich beams.

EXPERIMENTAL

Raw materials

Chlorinated butyl rubber (CIIR) used in this study is a commercial grade (HT-1066; Exxon); Petroleum resins

Correspondence to: C. F. Wu (wucf@ecust.edu.cn).

Journal of Applied Polymer Science, Vol. 106, 2472–2478 (2007)

TABLE I
Softening Points and Glass Transition Temperatures of Petroleum Resins in the Study

Code	Softening point (°C)	Glass transition temperature (°C)
P70	70	35
P100	100	58.5
P115	115	72
P140	140	86

(as shown in Table I) are commercial grade (Arakawa Chemical Industries).

Sample preparation

The CIIR were kneaded by mixing rollers for 5 min, and then the petroleum resin was added. The mixtures were pressed at 150°C for 10 min under a pressure of 10 MPa. The thickness of the prepared sheet was about 2 mm, and was used as the damping layer. Here, polyethylene terephthalate (PET) sheet was chosen as the constraining layer. Because of the self-adhesive property for the CIIR/petroleum resins blend, the constraining layer can be bonded with the CIIR/petroleum resins blends directly. The sandwich was achieved by pressing the constraining layer laminated with a damping layer under 0.2 MPa pressure at room temperature. The thickness of the damping layer was controlled by the pressing time, and three samples with different thicknesses and component were prepared as listed in Table II.

Dynamic mechanical analysis (DMA)

The viscoelastic properties of the blended CIIR were measured by the dynamic mechanical analyzer (Rheogel-E4000; UBM) on specimens of the following dimensions: 20 mm in length, 4 mm in width and 2 mm in thickness. The temperature dependence of tan δ was measured at a constant frequency of 11 Hz and at a heating rate of 3°C/min.

Because the damping layer undergoes pure shear in the sandwich structure, the dynamic mechanical properties of CIIR/petroleum resins blends under solid shear mode were measured with a strain set at 0.07%,[12] too. Specimens for the measurements were prepared as 6 mm in length, 6 mm in width, and 2 mm in thickness. The frequency dependence of dynamic shear modulus and loss tangent was measured from 1 Hz to 500 Hz at a series of temperatures.

DMA can measure the variation of loss factor of a material with many factors and has been widely used by researchers. Therefore, an attempt was made here to measure the vibration damping behaviors of sandwich beams by DMA. In practice, the ends of many apparatuses are fixed and there is a vibration in the middle of the body. So, the sandwich beam tested here has a boundary condition that both ends of the beam are clamped with a concentrated sinusoidal load $P_0e^{i\omega t}$ applied at the midpoint of the constraining layer as depicted in Figure 1, and the testing conditions are listed in Table II.

RESULTS AND DISCUSSION

Viscoelastic properties of chlorinated butyl rubber blends

Figure 2 shows the temperature dependence of the loss tangent (tan δ) at 11 Hz for various CIIR/petroleum resins samples. The content of petroleum resins for all of the samples remains constant at 150 phr. As shown in the figure, the CIIR/petroleum resins blends behave a single tan δ peak, which demonstrates that petroleum resins are compatible with CIIR, and the peak location shifts to higher temperatures with increasing the T_g of petroleum resins. Moreover, a broad and intense tan δ peak appears as shown in Figure 2. From this figure it can be seen that all the CIIR/petroleum resins blends show efficient damping (tan δ > 0.5) over a wide temperature range more than 74°C. Specifically, the CIIR/P70 blend exhibits high damping at room temperature (tan δ $= 1.85$ at 20°C), and shows efficient damping (tan δ > 0.5) over a wide temperature range from 0°C to 76°C ($\Delta T = 76$°C). Kerwin indicated that a higher loss tangent of viscoelastic

TABLE II
Dimensions and Testing Conditions of the Tested Samples

Sample code	Length (mm)	Width (mm)	Thickness (mm)		Composition of the damping layer	Composition of the constraining layer	Measuring temperature (°C)	Measuring frequency (Hz)
			Damping layer	Constraining layer				
1	30	4	0.10	1.22	CIIR/P70 (100/50)	PET	7–35	50 200 400
2	30	4	0.32	1.22	CIIR/P70 (100/50)	PET	7–35	50 200 400
3	30	4	0.32	1.22	CIIR/P70 (100/100)	PET	7–35	50 200 400

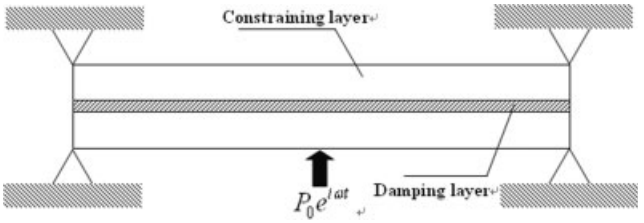

Figure 1 Sketch of the sandwich beam under a clamped-clamped boundary condition.

materials will conduce to the damping capacity of sandwich.[14] Therefore CIIR/P70 blends are selected as the damping layer and the variation of loss tangent with the composition of blends is shown in Figure 3.

For the comparison of the shear loss tangents values among various CIIR/P70 blends in a wide frequency range, the time–temperature superposition principle was used and the William–Landel–Ferry (WLF) equation was applied to obtain the master curves for the shear loss tangent over a wide frequency range. A series of measurements on frequency dependence of dynamic mechanical properties were performed at various temperatures near the corresponding glass transition temperature for CIIR/P70 blends. The testing frequencies for these measurements were in the range from 1 Hz to 100 Hz. In accordance with these results, the constants in the WLF equation were obtained as $C1 \approx 8.86$ and $C2 \approx 101.6$.

Figure 4 shows master curves of the shear loss tangent versus frequency for various CIIR/P70 samples with respect to a reference temperature of 25°C. From this figure, it can be seen that CIIR/P70 (100 : 150) has the highest damping peak, however, when the frequency is larger than 13 Hz, the loss tangent of CIIR/P70 (100 : 100) is higher than that of CIIR/P70 (100 : 150). Compared with CIIR/P70 (100 : 100), CIIR/P70 (100 : 50) has a higher damping capacity when the frequency is larger than 138 Hz, so CIIR/P70 (100 : 50) and CIIR/P70 (100 : 100) were selected as the damping layer of the sandwich beams.

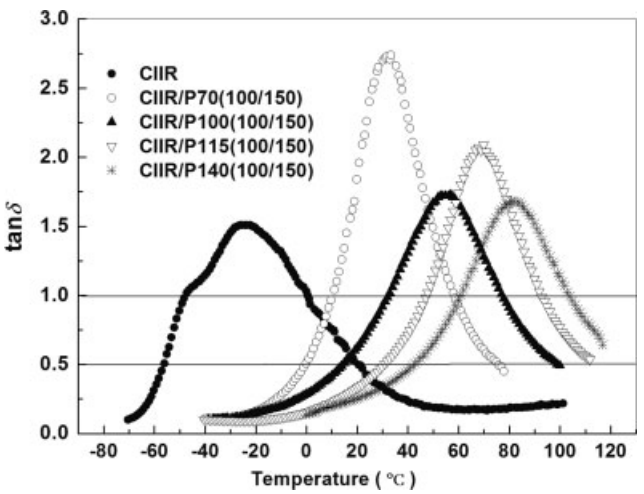

Figure 2 Temperature dependence of tan δ at 11 Hz for CIIR/petroleum resins (150 phr) blends.

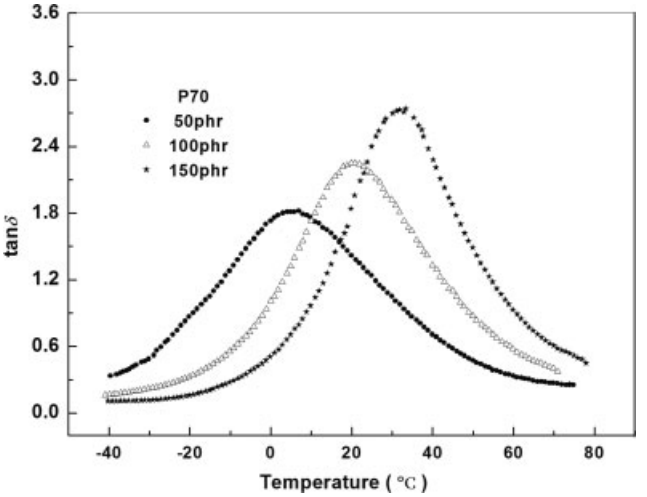

Figure 3 Temperature dependence of tan δ at 11 Hz for CIIR/P70 blends.

Vibration damping behaviors of sandwich beams

Figure 5 shows the variation of structural loss factor η_s with temperature for Sample 1 at different frequencies. It can be seen from this figure that the tendency of η_s with temperature is not the same at different frequencies. At 50 Hz, the η_s decreases with temperature, whereas the η_s keeps increasing with temperature at 400 Hz, and it increases at first then decreases with temperature at 200 Hz. This phenomenon indicates that the η_s of the sandwich beam is affected by temperatures and frequencies significantly. If 20°C is selected as the temperature for application, the damping capacity of the beam is higher at 200 Hz than those at other two frequencies.

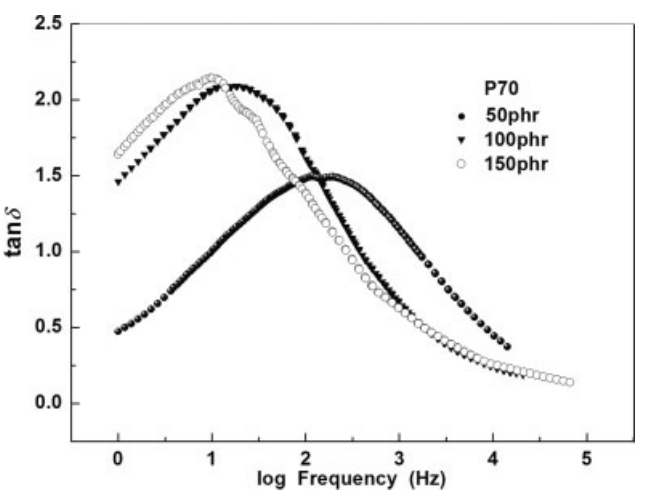

Figure 4 Frequency dependence of shear loss tangent for CIIR/P70 blends with reference temperature 25°C.

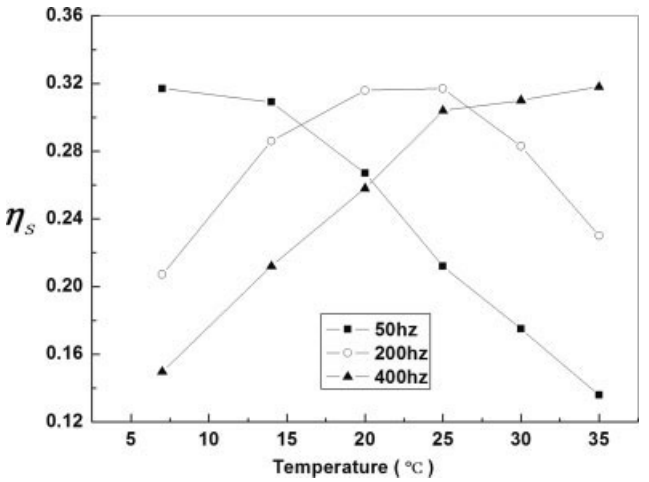

Figure 5 Variation of structural loss factor η_s with temperature for Sample 1 at different frequencies.

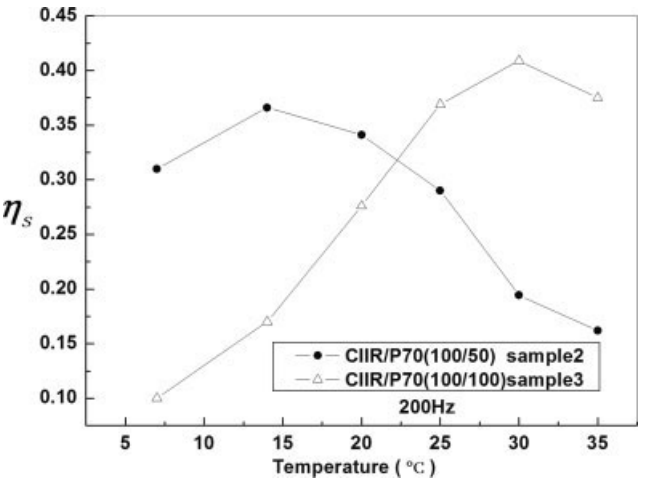

Figure 7 Variation of structural loss factor η_s with temperature for Sample 2 and Sample 3 with different composition at 200 Hz.

Figure 6 shows the variation of structural loss factor η_s with temperature for Samples 1 and 2 with different thickness of the damping layer at 200 Hz. In general, an increase in the thickness of the damping layer can lead to a higher structural loss factor. However, it can be seen from this figure that when the temperature is higher than 25°C, Sample 1 with thinner damping layer exhibits a higher damping capacity. In addition, the maximum structural loss factors appear at different temperatures because of the different thicknesses of the damping layers.

Figure 7 shows the variation of structural loss factor η_s with temperature for Samples 2 and 3 with different composition at 200 Hz. It can be seen from this figure that different viscoelastic materials lead to a quite different vibration damping behavior. This result suggests that to obtain a better damping capacity, CIIR/P70 (100 : 50) is more suitable when temperature is lower than 20°C, whereas CIIR/P70 (100 : 100) is preferential at temperatures higher than 25°C.

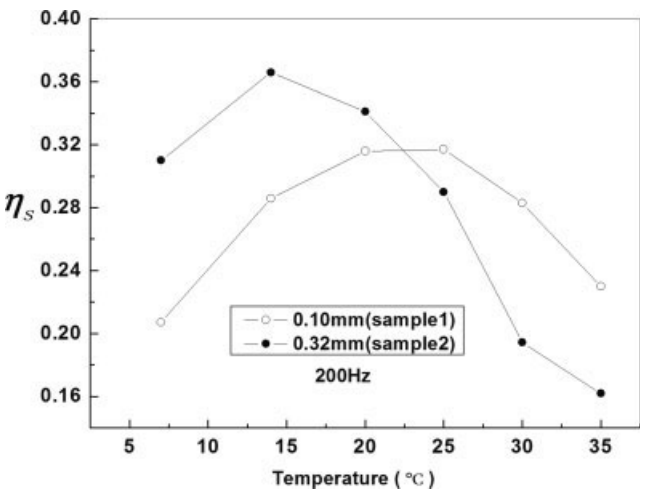

Figure 6 Variation of structural loss factor η_s with temperature for Sample 1 and Sample 2 with different thickness of the damping layer at 200 Hz.

DMA test results show that sandwich beams exhibit different vibration damping behaviors with the variation of temperature, frequency, and the thickness and composition of the damping layer. Though the method proposed here is different from the standard ASTM E 756-98, it can reflect the variation of structural loss factor with various factors. The correlation between the two methods will be investigated in future work.

Theoretical Analysis

To illustrate the phenomena mentioned above, a theoretical model was established. The damping of a system under steady state vibration can be expressed by the structural loss factor, which is the ratio of the energy dissipated per cycle to the maximum strain energy in the system.[11] That is,

$$\eta_S = \Delta W / 2\pi W_S \tag{1}$$

The calculation of ΔW could be done using an energy consuming model proposed by Plunkett.[15]

$$\Delta W = 2\pi h_2 E_2 L \varepsilon_0^2 \frac{1}{\omega} \left\{ \begin{array}{c} \sinh[\omega\ \cos(\theta/2)]\ \sin(\theta/2) \\ -\sin[\omega\ \sin(\theta/2)]\ \cos(\theta/2) \\ \hline \cosh[\omega\ \cos(\theta/2)] \\ +\cos[\omega\ \sin(\theta/2)] \end{array} \right\} \tag{2}$$

Where $\omega = \frac{L}{\sqrt{h_1 h_2 E_2 / G^*}}$, h_1 and h_2 are the thickness of the damping layer and the constraining layer respectively; E_2 is the modulus of elasticity of the constraining material; L is the length of the sandwich beam; G^* ($(G^* = \sqrt{(G')^2 + (G'')^2}\ )$) is the effective shear modu-

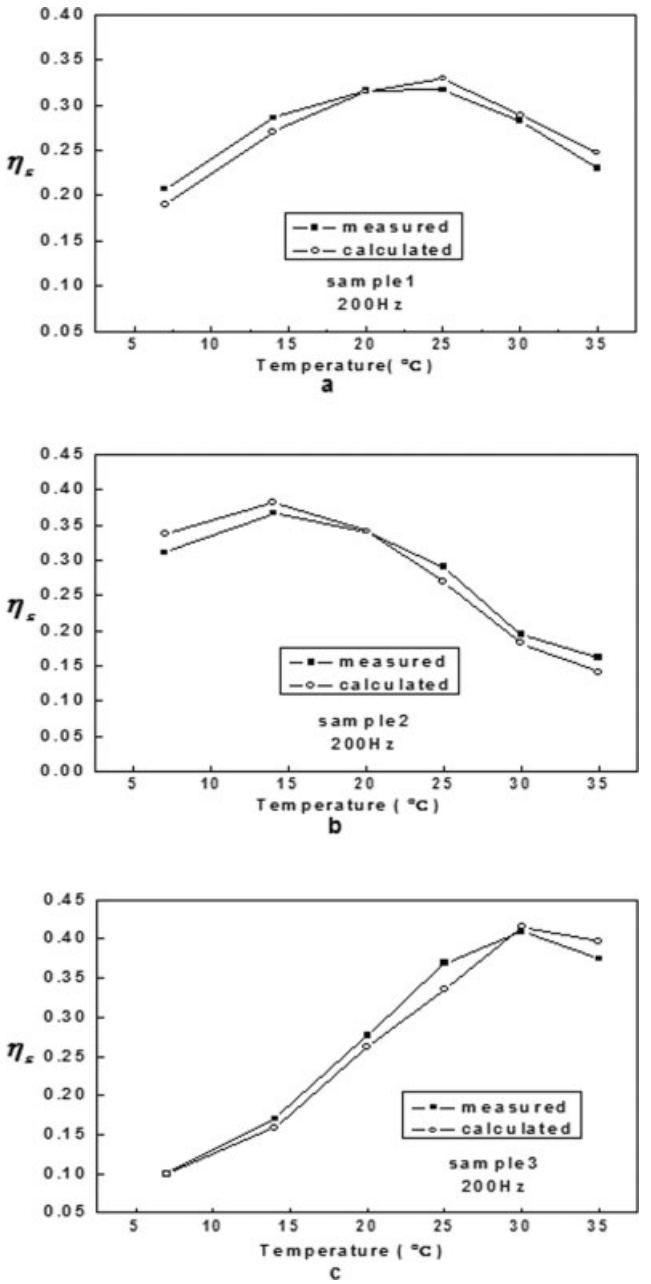

Figure 8 Measured values and calculated values versus temperature at 200 Hz.

lus of the viscoelastic material; ε_0 is the uniform strain at the interface of the base layer, and θ is the loss angle of the viscoelastic material ($\tan\theta = \tan\delta$).

The maximum strain energy in a constraining layer can be expressed as[16]

$$w_2 = \frac{E_2 I_2}{2}\int_0^L \left(\frac{d^2y}{dx^2}\right)^2 dx = \frac{E_2 {h_2}^3}{24}\int_0^L \left(\frac{d^2y}{dx^2}\right)^2 dx = \frac{E_2 {h_2}^3 L}{24}\frac{1}{{\rho_2}^2} \quad (3)$$

The maximum strain energy in a base layer has the similar formation

$$w_3 = \frac{E_3 I_3}{2}\int_0^L \left(\frac{d^2y}{dx^2}\right)^2 dx = \frac{E_3 {h_3}^3}{24}\int_0^L \left(\frac{d^2y}{dx^2}\right)^2 dx = \frac{E_3 {h_3}^3 L}{24}\frac{1}{{\rho_3}^2} \quad (4)$$

where I_2 and I_3 are moments of inertia of the constraining and base layer, respectively; ρ_2 and ρ_3 are curvature radii of the constraining and base layer, respectively. Because of the much lower modulus of the damping layer compared with that of the constraining layer, the maximum strain energy in the damping layer is negligible. Thus, the maximum strain energy of the system can be represented as:

$$W_S = w_2 + w_3 = \frac{E_2 {h_2}^3 L}{24}\frac{1}{{\rho_2}^2} + \frac{E_3 {h_3}^3 L}{24}\frac{1}{{\rho_3}^2} \quad (5)$$

Because the laminate is symmetric, the base layer is equal to the constraining layer, and $E_2 = E_3$, $h_2 = h_3$. Therefore,

$$W_S = w_2 + w_3 = \frac{E_2 {h_2}^3 L}{24}\left(\frac{1}{{\rho_2}^2} + \frac{1}{{\rho_3}^2}\right) \quad (6)$$

The strain at the interface of the base layer and the damping layer is

$$\varepsilon_0 = -(h_3/2)(d^2y/dx^2) = -(h_3/2)(1/\rho_3) \quad (7)$$

So eq. (2) can be written as:

$$\Delta W = 2\pi h_2 E_2 L\left({h_3}^2/4{\rho_3}^2\right)\frac{1}{\omega}\left\{\begin{array}{c}\sinh[\omega\cos(\theta/2)]\ \sin(\theta/2) \\ -\sin[\omega\sin(\theta/2)]\ \cos(\theta/2) \\ \hline \cosh[\omega\cos(\theta/2)] \\ +\cos[\omega\sin(\theta/2)]\end{array}\right\} \quad (8)$$

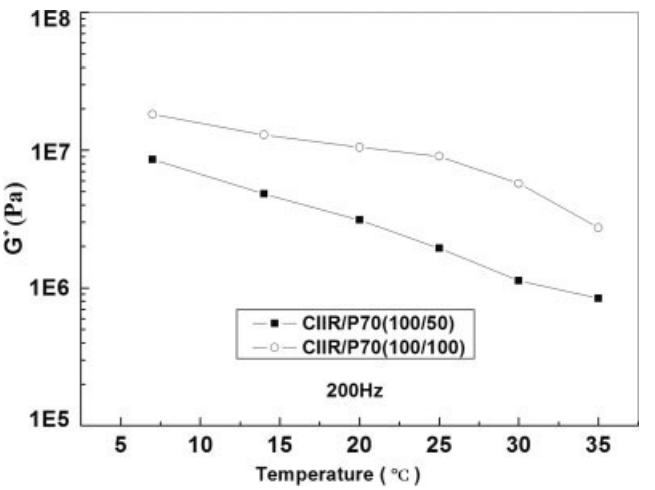

Figure 9 Temperature dependence of G^* at 200 Hz for CIIR/P70 blends.

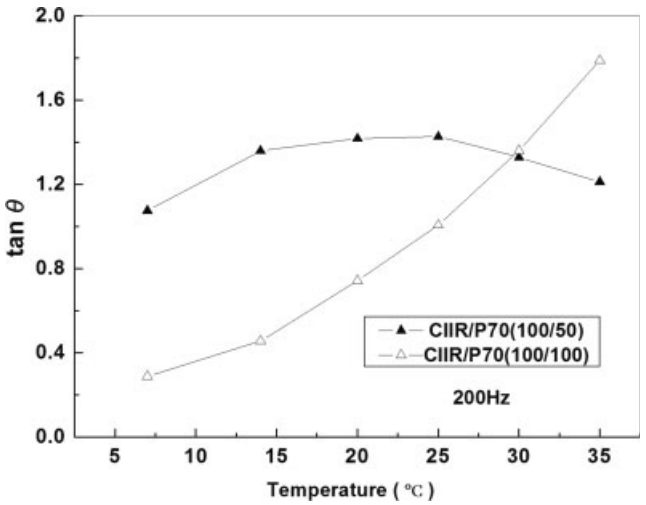

Figure 10 Temperature dependence of tan θ at 200 Hz for CIIR/P70 blends.

Substituting eqs. (8) and (6) into eq. (1), finally, the expression of the structural loss factor is obtained:

$$\eta_S = \Delta W/2\pi W_S = m\frac{1}{\omega}\left\{\frac{\sinh[\omega\cos(\theta/2)]\ \sin(\theta/2)}{-\sin[\omega\sin(\theta/2)]\ \cos(\theta/2)}\right\} \quad (9)$$

where, $m = \frac{6(1/\rho_3{}^2)}{(1/\rho_3{}^2+1/\rho_2{}^2)}$.

Figure 8 shows the measured values and calculated values based on eq. (9) versus temperature at 200 Hz. The G^* and tan θ of the damping layer materials used in eq. (9) at 200 Hz are shown in Figures 9 and 10, respectively. Because the storage modulus of the constraining layer is insensitive to the testing temperature, according to the DMA test data, the value is set to 1.6×10^9 Pa. An agreement between the measured values and the calculated values derived from eq. (9) can be found in Figure 8.

Figure 11 describes the variation of η_s with the shear modulus and loss angle of the damping layer materials for three samples based on eq. (9). Figure 11(a,b) shows the similar tendency that with the decrease of G^*, η_s increases at first, then decreases. However, it can be found that the values of G^* corresponding to the maximum η_s are different: G^* for sample 1 is 2.1×10^6 Pa, while G^* for sample 2 is 5.5×10^6 Pa. This means that for the maximum η_s to appear, Sample 1 with a thinner damping layer needs a lower shear modulus compared with Sample 2. Therefore, the maximum η_s of Sample 1 appearing at a higher temperature as shown in Figure 6 is easy to understand.

Figure 11(c) shows that a maximum η_s appears for Sample 3 when the G^* of the damping layer material reaches 4.4×10^6 Pa. Referring to Figure 9, it can be seen that the temperature corresponding to the modulus (4.4×10^6 Pa) of CIIR/P70 (100 : 100) is located near 30°C. Thus a high η_s will appear at 30°C, and the measured results shown in Figure 7 testify the prediction.

The discussion above proves that the vibration damping behaviors of sandwich beams can be explained to a certain extent using the model established here.

CONCLUSIONS

High damping materials were prepared by CIIR/petroleum resins blends. Petroleum resins are very effective for improving the damping ability of CIIR, especially P70 has the most excellent damping endowed

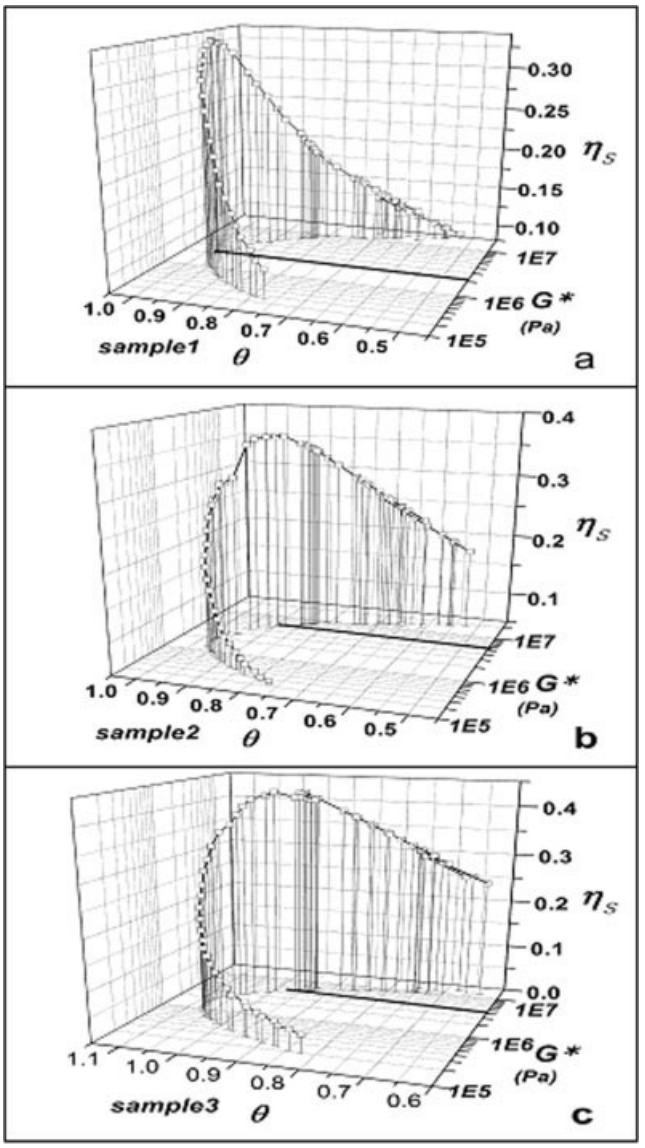

Figure 11 Variation of η_s with the shear modulus and the loss angle of the damping layer materials for three samples based on eq. (9).

function and CIIR/P70 blends were selected as the damping layers.

A new approach by DMA with a boundary condition that both ends of the beam are clamped with a concentrated sinusoidal load $P_0e^{i\omega t}$ applied at the midpoint of the constraining layer was used to measure the vibration damping behaviors of sandwich beams. Though this method is different from the standard ASTM E 756-98, it can reflect the variation of structural loss factor with various factors. On the other hand, because of the popular application of DMA, it has the possibility to become a new way to measure the vibration damping behaviors of sandwich structures.

References

1. Ting, R. Y.; Capps, R. N.; Klempner, D. Polym Mater Sci Eng 1989, 60, 654.
2. Li, S.; Peng, W; Lu, X. Int J Polym Mater 1995, 29, 37.
3. Wang, J.; Liu, R.; Li, W.; Li, Y.; Tang, X. Polym Int 1996, 39, 101.
4. Chen, Q. G.; Chen, D.; Yu, X. J Appl Polym Sci 1994, 54, 1191.
5. Wei, Z.; Li, S. J Appl Polym Sci 2002, 84, 821.
6. Corsaro, R. D.; Sperling, L. H. Sound and Vibration Damping with Polymers, ACS Symposium Series 424; American Chem Society: Washington, DC, 1990.
7. Wu, C. F.; Yamagishi, T.; Nakamoto, Y.; Ishida, S.; Nitta, K.; Kubota, S. J. Polym Sci Part B: Polym Phys 2000, 38, 1341.
8. Wu, C. F.; Yamagishi, T.; Nakamoto, Y.; Ishida, S.; Nitta, K.; Kubota, S. J Polym Sci Part B: Polym Phys 2000, 38, 1496.
9. Wu, C. F. J Appl Polym Sci 2001, 80, 2468.
10. Wu, C. F. J Non-Cryst Solids 2003, 315, 321.
11. Nashif, A. D.; Jones, D. I. G.; Henderson, J. P. Vibration Damping; Wiley: New York, 1985.
12. Liao, F. S.; Hsu, T. C. J Appl Polym Sci 1992, 45, 893.
13. Öborn, J.; Bertilsson, H.; Rigdahl, M. J Appl Polym Sci 2001, 80, 2865.
14. Kerwin, E. J Acoust Soc Am 1959, 31, 952.
15. Plunkett, R.; Lee, C. J Acoust Soc Am 1970, 48, 150.
16. Fan, Q. C.; Wang, B.; Yin, Y. J. Mechanics of Materials; Higher Education Press: Beijing, 2000.